OPEN ACCESS
OPUS AUGSBURG

Universität Augsburg
Universitätsbibliothek

Cross-presentation of dead-cell-associated antigens by DNGR-1+ dendritic cells contributes to chronic allograft rejection in mice

Saidou Balam, Rebecca Kesselring, Elke Eggenhofer, Stephanie Blaimer, Katja Evert, Matthias Evert, Hans J. Schlitt, Edward K. Geissler, Janneke van Blijswijk, Sonia Lee, Caetano Reis e Sousa, Stefan M. Brunner, Stefan Fichtner Feigl

Angaben zur Veröffentlichung / Publication details:

Balam, Saidou, Rebecca Kesselring, Elke Eggenhofer, Stephanie Blaimer, Katja Evert, Matthias Evert, Hans J. Schlitt, et al. 2020. "Cross-presentation of dead-cell-associated antigens by DNGR-1+ dendritic cells contributes to chronic allograft rejection in mice." *European Journal of Immunology* 50 (12): 2041–54. https://doi.org/10.1002/eji.201948501.

Nutzungsbedingungen / Terms of use: **CC BY 4.0**

Dieses Dokument wird unter folgenden Bedingungen zur Verfügung gestellt: / This document is made available under these conditions:
CC-BY 4.0: Creative Commons: Namensnennung
Weitere Informationen finden Sie unter: / For more information see:
https://creativecommons.org/licenses/by/4.0/deed.de

Check for updates

European Journal of Immunology

Transplantation and tolerance

Basic

Research Article

Cross-presentation of dead-cell-associated antigens by DNGR-1$^+$ dendritic cells contributes to chronic allograft rejection in mice

Saidou Balam[1], Rebecca Kesselring[1], Elke Eggenhofer[1], Stephanie Blaimer[1], Katja Evert[2], Matthias Evert[2], Hans J. Schlitt[1], Edward K. Geissler[1], Janneke van Blijswijk[4], Sonia Lee[4], Caetano Reis e Sousa[4], Stefan M. Brunner*[1] and Stefan Fichtner-Feigl*[1,3]*

[1] Department of Surgery, University Medical Center Regensburg, Regensburg, Germany
[2] Department of Pathology, University Medical Center Regensburg, Regensburg, Germany
[3] Department of General and Visceral Surgery, University Medical Center Freiburg, Freiburg, Germany
[4] Immunobiology Laboratory, The Francis Crick Institute, London, UK

The purpose of this study was to elucidate whether DC NK lectin group receptor-1 (DNGR-1)-dependent cross-presentation of dead-cell-associated antigens occurs after transplantation and contributes to CD8$^+$ T cell responses, chronic allograft rejection (CAR), and fibrosis. BALB/c or C57BL/6 hearts were heterotopically transplanted into WT, Clec9a$^{-/-}$, or Batf3$^{-/-}$ recipient C57BL/6 mice. Allografts were analyzed for cell infiltration, CD8$^+$ T cell activation, fibrogenesis, and CAR using immunohistochemistry, Western blot, qRT^2-PCR, and flow cytometry. Allografts displayed infiltration by recipient DNGR-1$^+$ DCs, signs of CAR, and fibrosis. Allografts in Clec9a$^{-/-}$ recipients showed reduced CAR ($p < 0.0001$), fibrosis ($P = 0.0137$), CD8$^+$ cell infiltration ($P < 0.0001$), and effector cytokine levels compared to WT recipients. Batf3-deficiency greatly reduced DNGR-1$^+$ DC-infiltration, CAR ($P < 0.0001$), and fibrosis ($P = 0.0382$). CD8 cells infiltrating allografts of cytochrome C treated recipients, showed reduced production of CD8 effector cytokines ($P < 0.05$). Further, alloreactive CD8$^+$ T cell response in indirect pathway IFN-γ ELISPOT was reduced in Clec9a$^{-/-}$ recipient mice ($P = 0.0283$). Blockade of DNGR-1 by antibody, similar to genetic elimination of the receptor, reduced CAR ($P = 0.0003$), fibrosis ($P = 0.0273$), infiltration of CD8$^+$ cells ($p = 0.0006$), and effector cytokine levels. DNGR-1-dependent alloantigen cross-presentation by DNGR-1$^+$ DCs induces alloreactive CD8$^+$ cells that induce CAR and fibrosis. Antibody against DNGR-1 can block this process and prevent CAR and fibrosis.

Keywords: CD8$^+$ T cells · cDC1 · cross-presentation · DNGR-1 · transplantation

Additional supporting information may be found online in the Supporting Information section at the end of the article.

Correspondence: Stefan M. Brunner
e-mail: Stefan.Brunner@ukr.de

*These authors contributed equally to this work.

© 2020 The Authors. *European Journal of Immunology* published by WILEY-VCH Verlag GmbH & Co. KGaA, Weinheim.
This is an open access article under the terms of the Creative Commons Attribution License, which permits use, distribution and reproduction in any medium, provided the original work is properly cited.

Introduction

Chronic rejection ultimately leading to allograft fibrosis and dysfunction constitutes a major constraint to long-term graft survival in transplantation [1–5]. In contrast to early post-transplant acute rejection episodes, which can be effectively treated with standard immunosuppressors to prevent activation and proliferation of alloreactive T lymphocytes, chronic rejection cannot be controlled sufficiently by these immunosuppressive therapies [6–9]. Activation of the immune system in the chronic setting is likely mediated through recognition of non-infectious damaged tissues [10–12]. This connection between cell injury and allograft rejection was proposed many years ago and posits that ischemia-reperfusion injury and other traumas during transplantation results in death of allograft cells, which expose intracellular molecules that trigger defensive immune responses in the host [13]. These intracellular molecules are termed damage-associated molecular patterns (DAMPs) and include molecules such as HMGB-1, ATP, uric acid, DNA, and others, which can in many instances engage innate immune receptors and promote inflammatory and adaptive immune responses [14,15].

DAMPs also include actin filaments, which can be recognized by the DC NK lectin group receptor-1 (DNGR-1, also known as CLEC9A) [16,17]. DNGR-1 is expressed by a subset of DCs in lymphoid and non-lymphoid tissues of mouse and human [18–24] that requires the Batf3 transcription factor for its development. The study of Batf3$^{-/-}$ mice lacking DNGR-1^{+} DCs (known as cDC1) has revealed that the latter play an essential and non-redundant role in CD8^{+} T cell responses against cell-associated antigens such as tumours and allografts, as well as against many viruses [24–26]. Interestingly, DNGR-1 serves not only as a marker for the Batf3-dependent cDC1 subset but appears to be required for its function as DNGR-1-deficient (Clec9a$^{-/-}$) mice recapitulate many of the functional defects of Batf3$^{-/-}$ mice despite the fact that their cDC1s develop normally. This is likely because F-actin engagement by DNGR-1 promotes cross-presentation of dead cell-associated antigens and cross-priming of cytotoxic CD8^{+} T cells (CTL) [16–19,27–29]. More specifically, F-actin-dependent DNGR-1 signaling facilitates the process whereby antigens associated with dead cell cargo taken up by cDC1 are shuttled into the MHC class I (MHC I) cross-presentation pathway. The latter includes the transporter associated with antigen processing 1 (Tap1) complex, which is essential for antigenic peptide translocation into the ER and, in synergy with other ER chaperones, for loading of the MHC I heavy chain/β-2-microglobulin (β2M) light chain complex [30–37].

Given the link between cell death and immunity to allotransplants, the present study aimed to test a possible involvement of DNGR-1 and of cDC1 in cross-priming CD8^{+} T cells against allograft antigens in a model of chronic rejection. Using a combination of genetic approaches and antibody blockade, we report that chronic allograft rejection and fibrosis can be prevented by inhibition of the DNGR-1 receptor and/or loss of DNGR-1^{+} DCs. These findings identify DNGR-1 as an important point of control in immunity to allotransplants that could be targeted therapeutically to ameliorate chronic allograft rejection.

Results

Cell necrosis in cardiac allografts exposes DAMPs and leads to infiltration by DNGR-1^{+} DCs

To investigate if cardiac allogeneity impacts early immune responses, BALB/c allografts transplanted into CD4^{+} T cell depleted C57BL/6 mice, which is a model of chronic allograft rejection and shows median allograft survival of 27 days, were evaluated by histology and RNA analysis at early times after transplantation (Fig. **1A**). Immunohistochemistry revealed early cell infiltration, and necrosis of cells within allografts (nucleus loss in cardiomyocytes, eosinophilic cytoplasms) at day 3 with further increases at day 5 after transplantation in comparison to syngeneic grafts (Fig. 1B; Supporting Information Fig. S1A and B). Additionally, in allografts, expression of death receptor and necrosis related genes such as TNF, myelin-associated glycoprotein (MAG), Fas ligand (Fasl), cytochromes, and CD40 was upregulated beginning at day 1 and increasing until day 5 after transplantation (Supporting Information Fig. S1C) [38–42]. This was accompanied by a higher CD11c^{+}DNGR-1^{+} DC infiltration of the allografts (BALB/c→C57BL/6) in comparison to syngrafts as demonstrated by double immunofluorescence staining (Fig. 1C and D; $p < 0.001$; Supporting Information Fig. S2). In contrast, no difference in DC subset composition was seen in the spleens of mice transplanted with allografts and syngrafts (Supporting Information Fig. S3).

Comparable to the results in mice, human cardiac allografts undergoing rejection showed greater leucocytic cell infiltration and collagen deposition at day 20 after transplantation than allografts without signs of rejection (Fig. 1E; mouse data, Fig. 3B and C). Notably, the human samples from rejecting hearts were infiltrated by CD11c^{+}DNGR-1^{+} DCs whereas these DCs were absent in human biopsies from healthy transplants (Fig. 1F and G; $p < 0.001$).

Graft-infiltrating DNGR-1^{+} cDC1s are of recipient origin and take up donor fragments

To elucidate if graft-infiltrating DNGR-1^{+} dendritic cells are of recipient or donor origin, we performed a triple immunofluorescence staining for H2^{b} (C57BL/6) and H2^{d} (BALB/c) in combination with CD11c and DNGR-1. This staining showed that graft-infiltrating DNGR-1^{+} DCs are H2^{b} and not H2^{d} positive in immunofluorescence staining and therefore are of C57BL6 recipient origin (Fig. 2A and B). The highest numbers of these graft-infiltrating DNGR-1^{+} DCs can be found on day 5 after transplantation with a decrease till day 20 after transplant (Fig. 2C). At both time points, no H2^{d} positive DNGR-1^{+} DCs that would indicate passenger DCs from BALB/c origin were detected.

© 2020 The Authors. *European Journal of Immunology* published by WILEY-VCH Verlag GmbH & Co. KGaA, Weinheim.

15214141, 2020, 12, Downloaded from https://onlinelibrary.wiley.com/doi/10.1002/eji.201948501 by Open Access University of Augsburg - Universitätsbibliothek Augsburg , Wiley Online Library on [04/05/2026]. See the Terms and Conditions (https://onlinelibrary.wiley.com/terms-and-conditions) on Wiley Online Library for rules of use; OA articles are governed by the applicable Creative Commons License

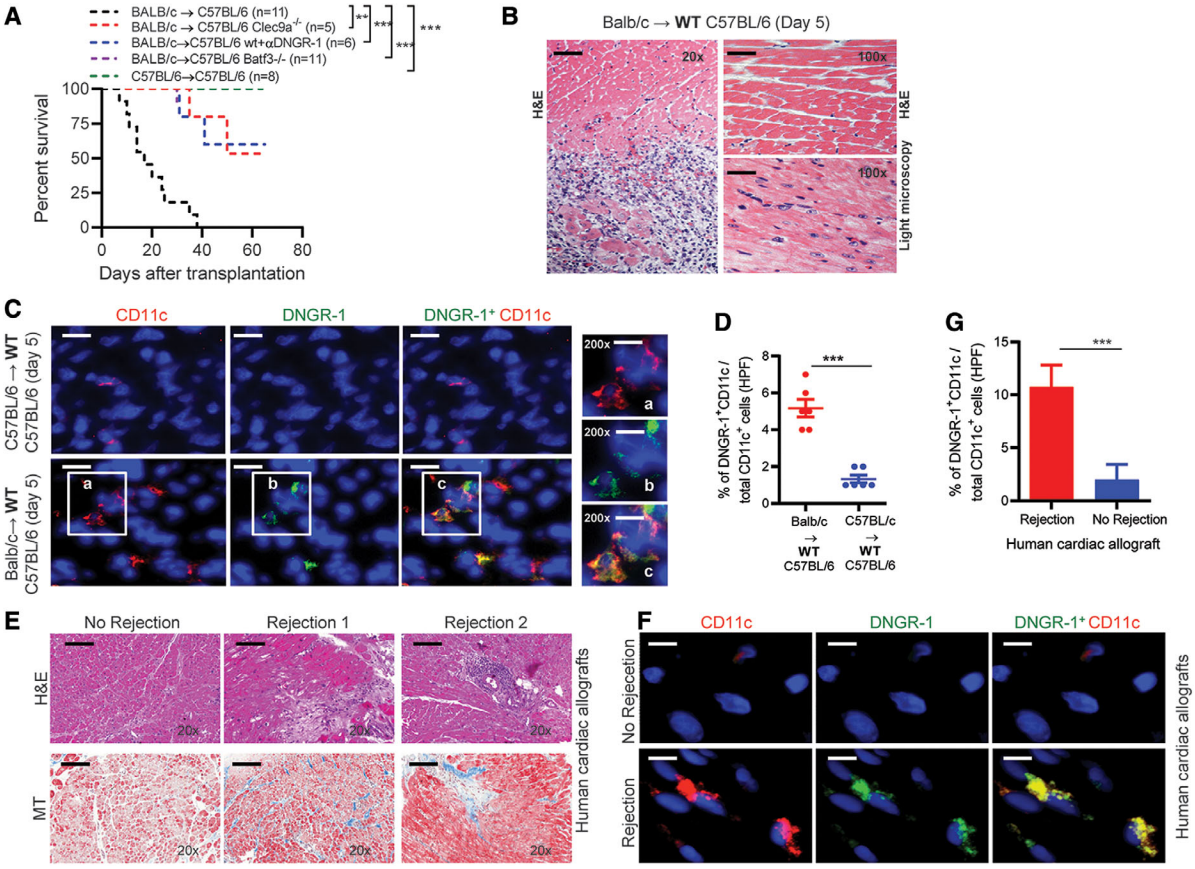

Figure 1. DNGR-1$^+$ DCs infiltrate mouse cardiac allografts and human cardiac allografts undergoing chronic rejection. **(A)** Wild-type (WT) C57BL/6 recipients were transplanted with BALB/c donor hearts (BALB/c → WT C57BL/6, allografts; $n = 11$) with a median graft survival time of 27 days which was significantly shorter when compared to syngeneic controls (C57BL/6 → WT C57BL/6, syngrafts; $n = 8$; $p < 0.0001$). CD4$^+$ T cells were depleted in all recipients. Further, *Clec9a*$^{-/-}$ ($n = 5$; $p < 0.01$), *Batf3*$^{-/-}$ ($n = 11$; $p < 0.001$), and α-DNGR-1 ($n = 6$; $p < 0.001$) treated C57BL/6 recipients transplanted with BALB/c donor hearts showed significantly prolonged allograft survival. **(B)** On day 5, cell infiltration (eosinophilia) and necrosis of cells within the allografts (nucleus loss in cardiomyocytes) were evaluated in H&E and light microscopy. Scale bar 100 μm, magnification 20× and 100×. **(C)** Allogeneic (BALB/c → WT C57BL/6) and syngeneic cardiac transplants (C57BL/6 → WT C57BL/6) were analyzed on day 5 post transplantation. Representative immunofluorescence (IF)-staining shows DNGR-1$^+$CD11c cell (DNGR-1$^+$ dendritic cell, DNGR-1$^+$ DC) within the allografts compared to the syngrafts. The double positive cells for DNGR-1 (green) and CD11c (red) are in yellow; nucleus is stained in blue. Scale bar 50 μm in magnification 40× and Scale bar 10 μm in magnification 200×. **(D)** Quantification of DNGR-1$^+$CD11c/total positive CD11c cells per high power field (HPF) within the allografts (BALB/c → WT C57BL/6) on day 5 compared to syngrafts (C57BL/6→WT C57BL/6) is depicted ($n = 6$ per group; shown as mean ± SD; Student's *t*-test). Error bars represent mean ± SD. **(E)** Paraffin-embedded human heart allografts (Rejection 1, 2, and No Rejection as control) were obtained. Representative H&E-staining of cell infiltration (upper panel) and Masson´s Trichrome (MT)-staining of collagen deposition (in blue, lower panel) within the rejection (1, 2) compared to the no rejected allografts are illustrated. Scale bar 100 μm, magnification 20×. **(F and G)** Representative IF-staining and quantification of DNGR-1$^+$ DCs (DNGR-1$^+$ CD11c in yellow; nucleus in blue) in the Rejection (lower panel) compared to the No Rejection groups (upper panel) is illustrated. Scale bar 50 μm, magnification 40×. (A–F) Data are from two experiments with four to six mice per experiment. Reactive oxygen species, ROS; Tumor necrosis factor, TNF; Myelin-associated glycoprotein, MAG; Fas ligand, Fasl; cytochromes, Cyba, Cybb; CD40; ***$p \leq 0.001$; paired Student's *t*-test.

However, we were able to depict H2^d positive BALB/c donor fragments (not DNGR-1 or CD11c positive) in cytoplasm of DNGR-1$^+$ DCs (Fig. 2D).

Absence of DNGR-1 reduces chronic rejection, allograft fibrosis, and CD8$^+$ T cell infiltration

Since DNGR-1$^+$ cDC1s infiltrated allografts but not syngrafts, we tested whether genetic abrogation of the DNGR-1 receptor could prevent chronic allograft rejection and fibrosis. Indeed, Clec9a$^{-/-}$ recipient mice that are deficient for the DNGR-1 receptor [27] showed significantly prolonged allograft survival ($p < 0.01$; Fig. 1A), decreased immune cell infiltration and histology rejection score of allografts compared to WT recipients ($p < 0.0001$; Fig. 3A). This was accompanied by a significant reduction of collagen I deposition in allografts both in Masson's trichrome staining and PCR ($p = 0.0137$; Fig. 3B). Further, profibrotic cytokines such as active TGF-β1 ($p = 0.0043$) and CTGF ($p = 0.0040$) were detected at significantly reduced levels in allotransplanted Clec9a$^{-/-}$ compared to WT recipient mice (Fig. 3C). These results were corroborated by immunofluorescent detection of phosphorylated Smad3 in allografts transplanted into WT recipient animals but not into Clec9a$^{-/-}$ mice (Fig. 3D).

© 2020 The Authors. *European Journal of Immunology* published by WILEY-VCH Verlag GmbH & Co. KGaA, Weinheim.

15214141, 2020, 12, Downloaded from https://onlinelibrary.wiley.com/doi/10.1002/eji.201948501 by Open Access University of Augsburg - Universitätsbibliothek Augsburg , Wiley Online Library on [04/05/2026]. See the Terms and Conditions (https://onlinelibrary.wiley.com/terms-and-conditions) on Wiley Online Library for rules of use; OA articles are governed by the applicable Creative Commons License

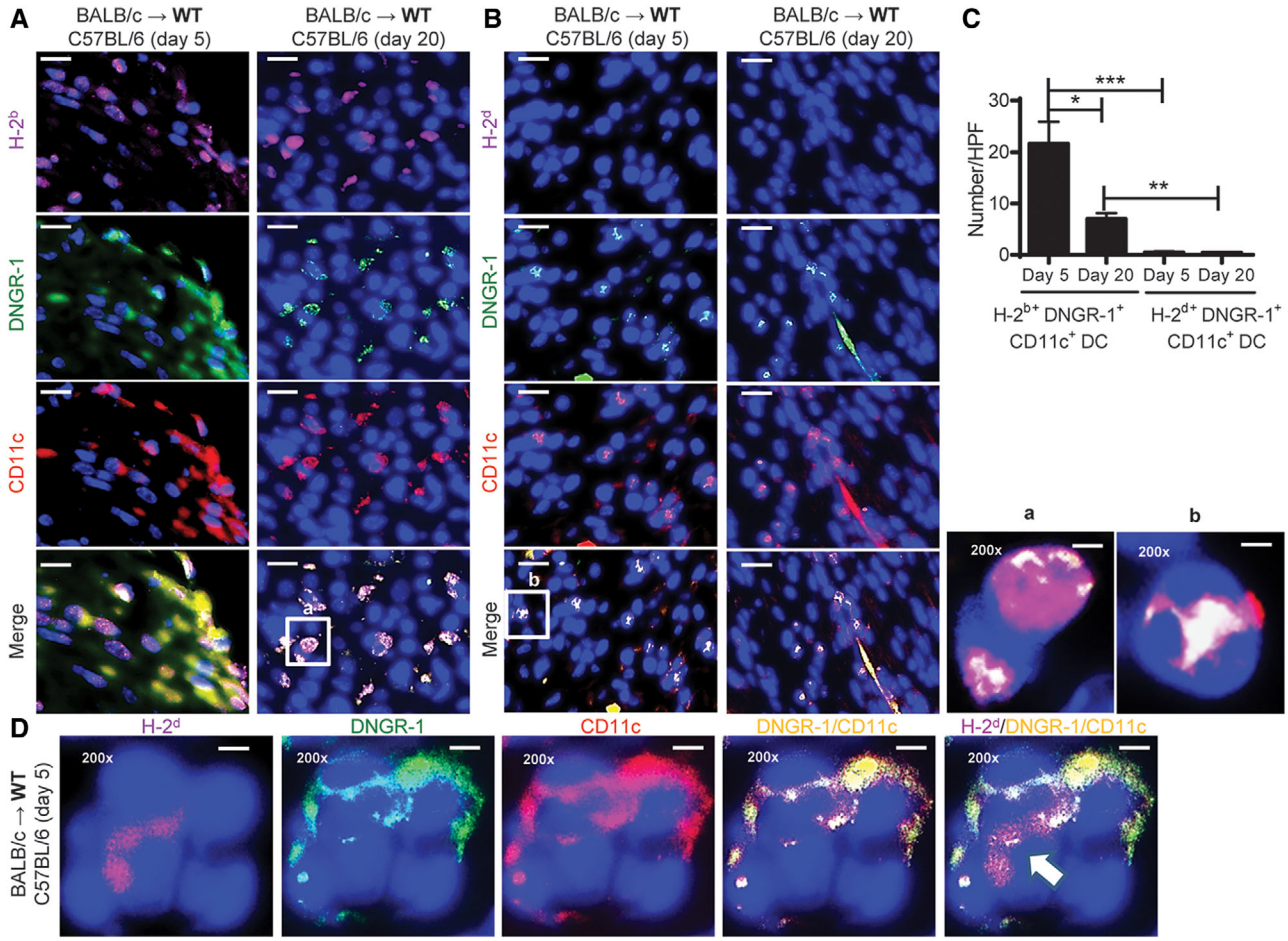

Figure 2. Graft-infiltrating DNGR-1$^+$ cDC1s are of recipient origin and take up donor fragments. Wild-type C57BL/6 recipient were transplanted on day 0 with BALB/c donor hearts (BALB/c → WT C57BL/6, allografts). Grafts harvested on day 5 and day 20 were analyzed to determine the origin of DNGR-1$^+$ DC (DNGR-1$^+$CD11c$^+$) within the allografts. **(A)** Representative IF-staining showing recipient origin of DNGR-1$^+$ DCs with positivity for H-2^b (H-2^{b+} DNGR-1$^+$ DC, in violet, nuclei in blue; (a) higher magnification (×200)) in allografts at day 5 and day 20 after transplantation. Scale bar 50 μm, magnification 40×. **(B)** Representative IF-staining showing DNGR-1$^+$ DCs (DNGR-1$^+$ CD11c$^+$ in yellow or orange, nuclei in blue; (b) higher magnification (×200)) with absence of H-2^{d+} (donor BALB/c origin) in allografts at day 5 and day 20 after transplantation. Scale bar 50 μm, magnification 40×. **(C)** Quantification (mean ± SD; Mann–Whitney *U*-test) per HPF (graph) of H-2^{b+} DNGR-1$^+$ DCs (recipient origin) and H-2^{d+} DNGR-1$^+$ DCs (donor origin) within the allografts at day 5 ($n = 4$) compared to day 20 after transplantation ($n = 4$). **(D)** Representative IF-staining showing H-2^d expressing donor fragments (in magenta; white arrow) surrounded by DNGR-1$^+$ CD11c$^+$ DCs (in yellow); allograft was harvested on day 5. Scale bar 10 μm, magnification 200×. (A–D) Data are from two independent experiments with four to six mice per experiment. $^*p < 0.05$; $^{**}p < 0.01$; $^{***}p < 0.001$.

In Clec9a$^{-/-}$ mice, numbers of allograft infiltrating CD8$^+$ T cells were significantly reduced in comparison to WT recipients or mice receiving syngeneic grafts ($p < 0.0001$; Fig. 4A). This was accompanied by a significant reduction of CD8 effector cytokines IFN-γ and IL-33 in the Clec9a$^{-/-}$ animals (IFN-γ $p = 0.0151$, IL-33 $p < 0.0001$; Fig. 4B) while trafficking of cDC1s into the allograft was not impaired (Supporting Information Fig. S4).

Batf3 is necessary for chronic allograft rejection

It is described previously that the development of DNGR-1 expressing cDC1s is dependent on the transcription factor Batf3 [24, 25]. Indeed, leucocytic cell infiltration was significantly decreased in Batf3$^{-/-}$ mice receiving allografts when compared to WT recipients ($p < 0.0001$; Fig. **5A**; Supporting Information Fig. S4) and allograft survival was prolonged significantly ($p < 0.001$; Fig. 1A). Absence of Batf3 in recipient mice also prevented collagen deposition in the allografts as shown both by Masson's trichrome staining and PCR ($p = 0.0382$; Fig. 5B), as well as the induction of profibrotic cytokines and activation of Smad3 ($p = 0.0132$; CTGF $p = 0.0352$; Fig. 5C and D). As expected, the population of DNGR-1$^+$ cDC1s infiltrating allografts was significantly reduced in Batf3$^{-/-}$ mice (Supporting Information Fig. S5A) and was associated with a paucity of activated CD8$^+$ T cells ($p < 0.0001$; Supporting Information Fig. S5B) and RT-PCR levels of effector cytokines (IFN-γ $p < 0.0001$, IL-33 $p = 0.0250$; Supporting Information Fig. S5C).

© 2020 The Authors. *European Journal of Immunology* published by WILEY-VCH Verlag GmbH & Co. KGaA, Weinheim.

15214141, 2020, 12, Downloaded from https://onlinelibrary.wiley.com/doi/10.1002/eji.201948501 by Open Access University of Augsburg - Universitätsbibliothek Augsburg , Wiley Online Library on [04/05/2026]. See the Terms and Conditions (https://onlinelibrary.wiley.com/terms-and-conditions) on Wiley Online Library for rules of use; OA articles are governed by the applicable Creative Commons License

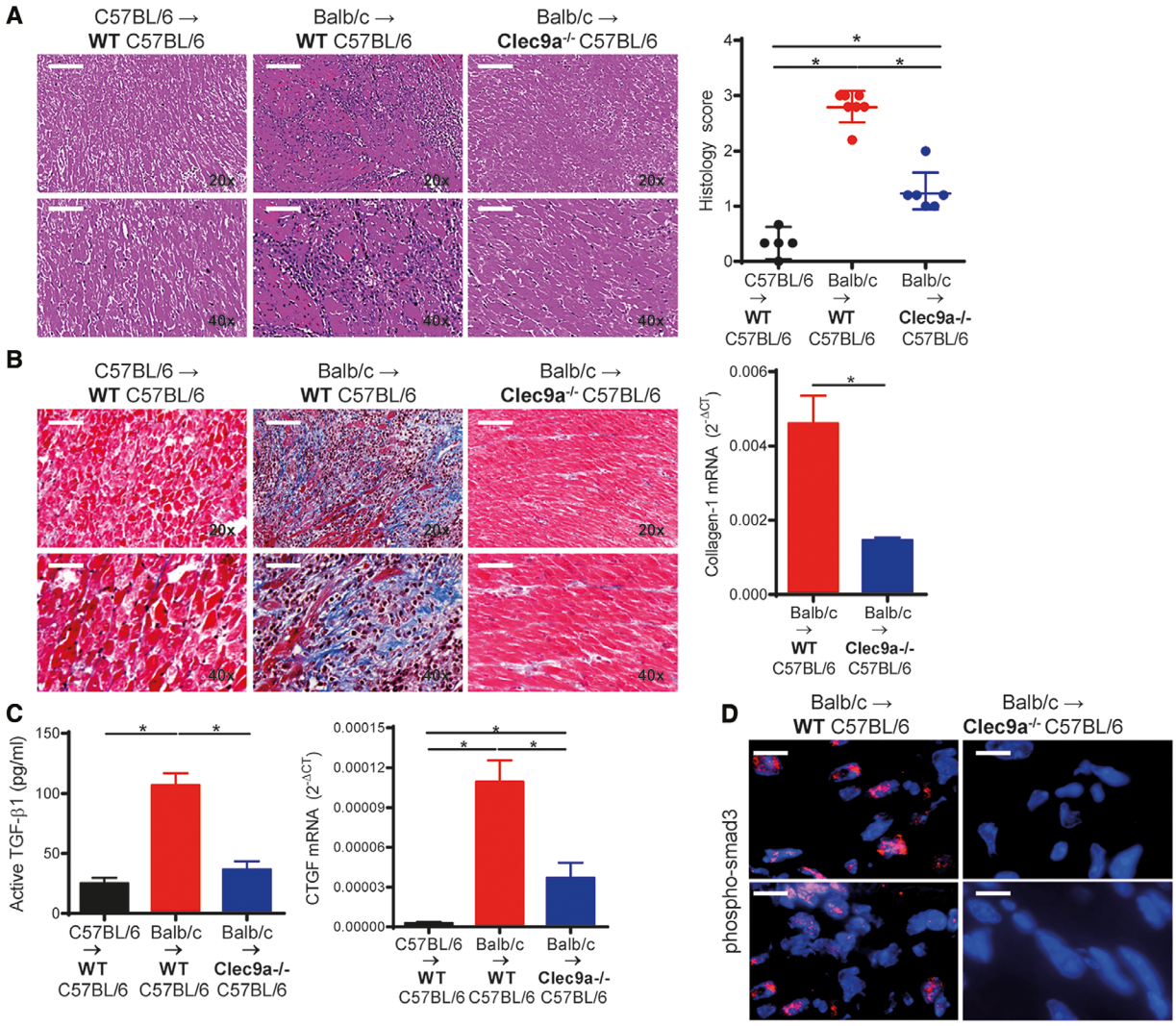

Figure 3. DNGR-1 deficiency in recipient mice prevents chronic rejection of cardiac allografts and fibrosis. Wild-type (WT) and DNGR-1 deficient (*Clec9a*$^{-/-}$) C57BL/6 recipients were transplanted on day 0 with BALB/c donor hearts (BALB/c → WT C57BL/6 and BALB/c → *Clec9a*$^{-/-}$ C57BL/6, allogeneic transplants). Control C57BL/6 recipient were transplanted with C57BL/6 donor hearts (C57BL/6 → WT C57BL/6, syngeneic transplants). Recipient mice were depleted of CD4$^+$ T cells with anti-CD4 antibody, i.p. (1 mg/mouse) on days -1, 0, and 7 and mice were analyzed on day 20 (n = 5–10 per group). **(A)** Representative H&E-staining of cell infiltration within the allografts and histology score of the allogeneic transplants into the *Clec9a*$^{-/-}$ C57BL/6 recipients compared to the transplants into WT C57BL/6 recipients and syngeneic transplants. Scale bar 100 μm in 20× magnification and Scale bar 50 μm in 40× magnification. **(B)** Masson's Trichrome-staining shows collagen deposition (in blue) within the allografts into *Clec9a*$^{-/-}$ C57BL/6 compared to the WT C57BL/6 recipients or syngrafts. Collagen mRNA expression within the allografts into *Clec9a*$^{-/-}$ C57BL/6 compared to WT C57BL/6 recipients is depicted (graph; n = 6 per group). Scale bar 100 μm in 20× magnification and Scale bar 50 μm in 40× magnification. **(C)** Determination of active TGF-β_1 and CTGF mRNA expression within the allogeneic transplants into *Clec9a*$^{-/-}$ C57BL/6 compared to WT C57BL/6 recipients or syngrafts are illustrated (n = 6 per group). **(D)** Representative IF -staining of phosphorylated smad3 (Phospho-Smad3, in red) within the allografts into *Clec9a*$^{-/-}$ C57BL/6 compared to WT C57BL/6 is depicted. Scale bar 50 μm, magnification 40×. (A–D) Data are from two independent experiments and are shown as mean ± SD and unpaired one-tailed Student's t-test was applied to compare two groups. *$P \leq 0.05$.

Selective apoptosis and DNGR1$^{-/-}$ reduces CD8$^+$ T cell allorecognition and allograft rejection

To formally assess the CD8 T cell alloimmune response within our model in vivo, we performed additional experiments with cytochrome C injection of recipient mice. In previous functional studies, both in vivo and in vitro it has been shown that cytochrome c profoundly abrogates OVA-specific CD8 T cell proliferation through its apoptosis-inducing effect on cross-presenting DCs [43]. In these experiments, in vivo injection of cytochrome C abolished the induction of cytotoxic T lymphocytes to exogenous antigen and reduced subsequent immunity to tumor challenge. Importantly, this model allows assessment of cross-presentation that is totally in vivo that is ideal for our setting of alloimmunity in transplantation [43].

In detail, we injected C57BL/6 recipient mice that were transplanted with BALB/c hearts with three dosages of cytochrome C and analyzed analogous to our original experiments.

© 2020 The Authors. *European Journal of Immunology* published by WILEY-VCH Verlag GmbH & Co. KGaA, Weinheim.

15214141, 2020, 12, Downloaded from https://onlinelibrary.wiley.com/doi/10.1002/eji.201948501 by Open Access University of Augsburg - Universitätsbibliothek Augsburg , Wiley Online Library on [04/05/2026]. See the Terms and Conditions (https://onlinelibrary.wiley.com/terms-and-conditions) on Wiley Online Library for rules of use; OA articles are governed by the applicable Creative Commons License

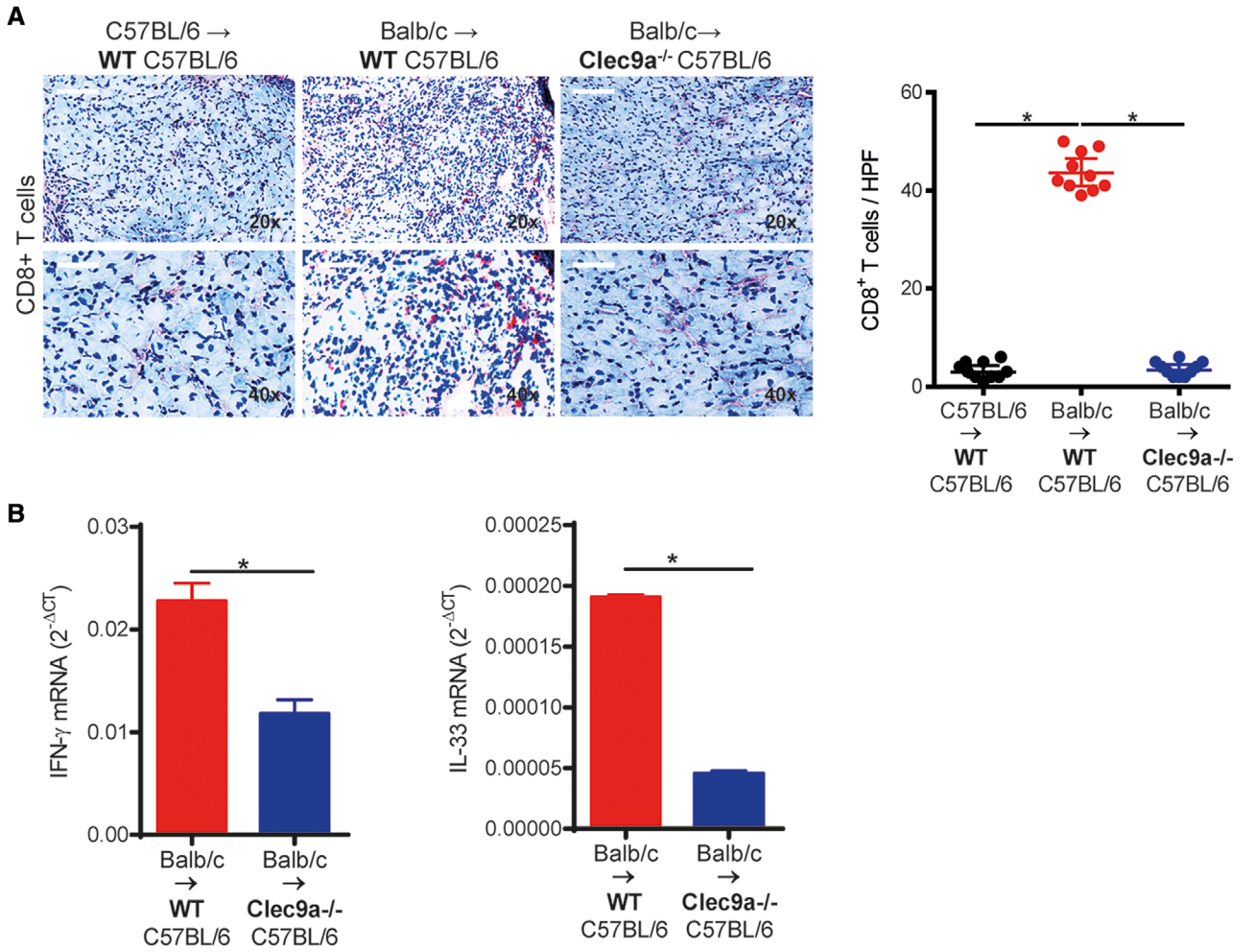

Figure 4. DNGR-1 deficiency in recipient mice prevents infiltration by CD8$^+$ T cells. Infiltration by CD8$^+$ T cells and effector cytokine expression within heart transplants using the same experimental setup as in Figure 3. (**A**) Immunohistochemical (IHC) staining showing infiltration of CD8$^+$ T cells (positive cells are in brown) and their quantification per high power field (HPF; graph on the right) within allogeneic transplants into *Clec9a*$^{-/-}$ C57BL/6 compared to WT C57BL/6 recipients or syngeneic transplants (n = 5–10 per group). Scale bar 100 μm in 20× magnification and Scale bar 50 μm in 40× magnification. (**B**) Quantification of mRNA expression (normalized against housekeeping gene β-actin)of effector cytokines (IFN-γ and IL-33) within the allogeneic transplants into *Clec9a*$^{-/-}$ C57BL/6 compared to WT C57BL/6 recipients (n = 5–10 per group). (A and B) Data are from two independent experiments and are shown as mean ± SD and unpaired one-tailed Student's t-test was applied to compare two groups. $^*p \leq 0.05$.

Cytochrome C injected recipient mice showed significantly decreased immune cell infiltration and histology rejection score of allografts compared to WT recipients (p = 0.0055; Supporting Information Fig. S6A). This was accompanied by a significant reduction of collagen I deposition in allografts both in Masson's trichrome staining and PCR (p = 0.0152; Supporting Information Fig. S6B) and also reduced CTGF levels (p = 0.0260; Supporting Information Fig. S6C). These results were corroborated by immunofluorescent detection of phosphorylated Smad3 in allografts transplanted into WT recipient animals but not into cytochrome c injected mice (Supporting Information Fig. S6D).

Further the numbers of DNGR-1$^+$ cDC1s infiltrating allografts were significantly reduced in cytochrome C-treated mice (p = 0.0116; Fig. 6A) and was associated with decreased numbers of activated CD8$^+$ T cells (p = 0.0097; Fig. 6B). CD8$^+$ T cells isolated out of allografts transplanted into cytochrome C-treated recipient mice, showed significant reduced production of CD8 T effector cytokines IFN-γ, TNF-α (and IL-2, IL-4, IL-13, and also the cytotoxic marker perforine 1; data not shown; all $p < 0.05$; Fig. 6C). Further, IFN-γ response by CD8$^+$ T cells in an indirect pathway Elispot was significantly decreased in Clec9a$^{-/-}$ compared to WT recipient mice (p = 0.0283; Fig. 6D).

Additionally, in all our experimental groups that show reduced allograft rejection due to either reduced BATF3 dependent DCs or impaired DNGR-1 receptor function (Cleac9a$^{-/-}$ and DNGR-1 antibody treated mice) reduced IFN-γ levels were detected. This altogether underlines that indeed DNGR-1$^+$ DCs cross-prime CD8$^+$ T cells and that these primed CD8 T cell effector responses contribute to allograft rejection and fibrosis.

© 2020 The Authors. *European Journal of Immunology* published by WILEY-VCH Verlag GmbH & Co. KGaA, Weinheim.

15214141, 2020, 12, Downloaded from https://onlinelibrary.wiley.com/doi/10.1002/eji.201948501 by Open Access University of Augsburg - Universitätsbibliothek Augsburg , Wiley Online Library on [04/05/2026]. See the Terms and Conditions (https://onlinelibrary.wiley.com/terms-and-conditions) on Wiley Online Library for rules of use; OA articles are governed by the applicable Creative Commons License

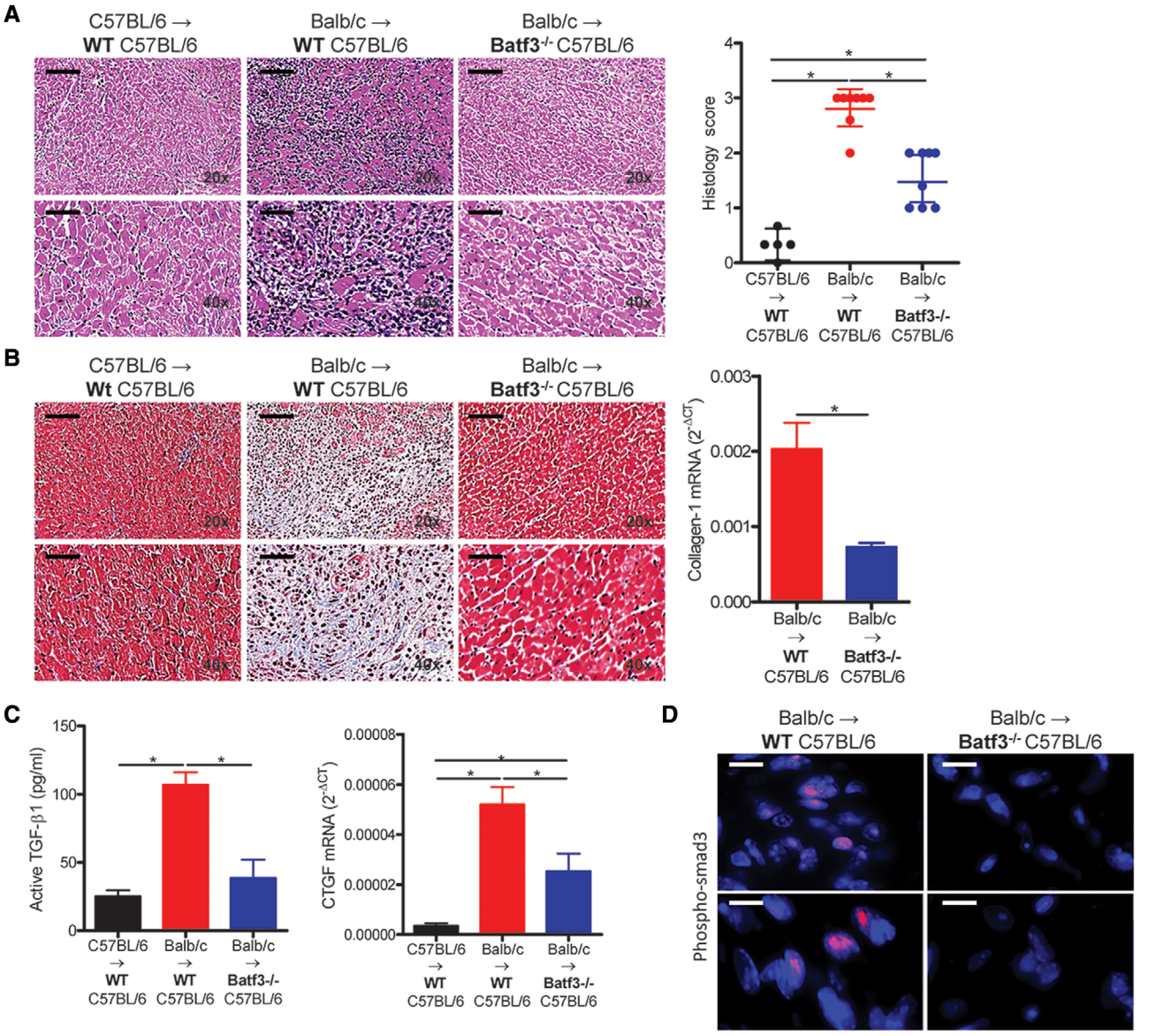

Figure 5. Batf3 deficiency in recipients reduces fibrosis and chronic rejection of allografts. Wild-type and Baft3$^{-/-}$ C57BL/6 recipients were transplanted with BALB/c donor hearts (BALB/c → WT C57BL/6 or Baft3$^{-/-}$ C57BL/6, allogeneic) and with C57BL/6 donor hearts (C57BL/6 → WT C57BL, syngeneic) and analyzed on day 20 ($n = 5$–8 per group). All recipients were depleted of CD4$^+$ T cells. **(A)** H&E staining shows cell infiltration within the allografts and histology score of allografts of the Batf3$^{-/-}$ C57BL/6 compared to WT C57BL/6 recipients or syngraft groups. Scale bar 100 μm in 20× magnification and Scale bar 50 μm in 40× magnification. **(B)** Deposition in MT (in blue) and mRNA expression (normalized against housekeeping gene β-actin) of collagen within the allografts of Batf3 deficient compared to WT recipient or syngeneic transplants are depicted. Scale bar 100 μm in 20× magnification and Scale bar 50 μm in 40× magnification. **(C)** Levels of active TGF-β_1 and mRNA expression of CTGF within the allografts of Batf3$^{-/-}$ C57BL/6 compared to the WT groups and syngrafts are shown. **(D)** Immunofluorescence-staining of Phospho-smad3 (red, nucleus in blue) in allografts of the Batf3$^{-/-}$ C57BL/6 compared to WT recipients is shown. Scale bar 50 μm, magnification 40×. (A–D) Data are from two independent experiments and are shown as mean ± SD and unpaired one-tailed Student's *t*-test was applied to compare two groups. $^*p \leq 0.05$.

Blockade of DNGR-1 receptor prevents chronic allograft rejection and fibrosis

Finally, blockade of DNGR-1 with specific mAb was tested for the ability to phenocopy genetic loss in allograft recipients and diminish chronic allograft rejection and fibrosis. Notably, mAb treatment significant prolonged allograft survival ($p < 0.0001$; Fig. 1A), reduced numbers of allograft-infiltrating cells ($p = 0.0003$; Fig. 7A) and collagen I deposition into allografts (P = 0.0273; Fig. 7B). Similar to genetic disruption of Clec9a, the profibrotic cytokines were significantly reduced in mAb treated compared to the control group (active TGF-β_1 $p = 0.0035$; CTGF $p = 0.0267$; Fig. 7C). Further, mAb treatment significantly reduced the infiltration of allografts by CD8$^+$ T cells ($p = 0.0006$; Fig. 7D), as well as the

© 2020 The Authors. *European Journal of Immunology* published by WILEY-VCH Verlag GmbH & Co. KGaA, Weinheim.

15214141, 2020, 12, Downloaded from https://onlinelibrary.wiley.com/doi/10.1002/eji.201948501 by Open Access University of Augsburg - Universitätsbibliothek Augsburg , Wiley Online Library on [04/05/2026]. See the Terms and Conditions (https://onlinelibrary.wiley.com/terms-and-conditions) on Wiley Online Library for rules of use; OA articles are governed by the applicable Creative Commons License

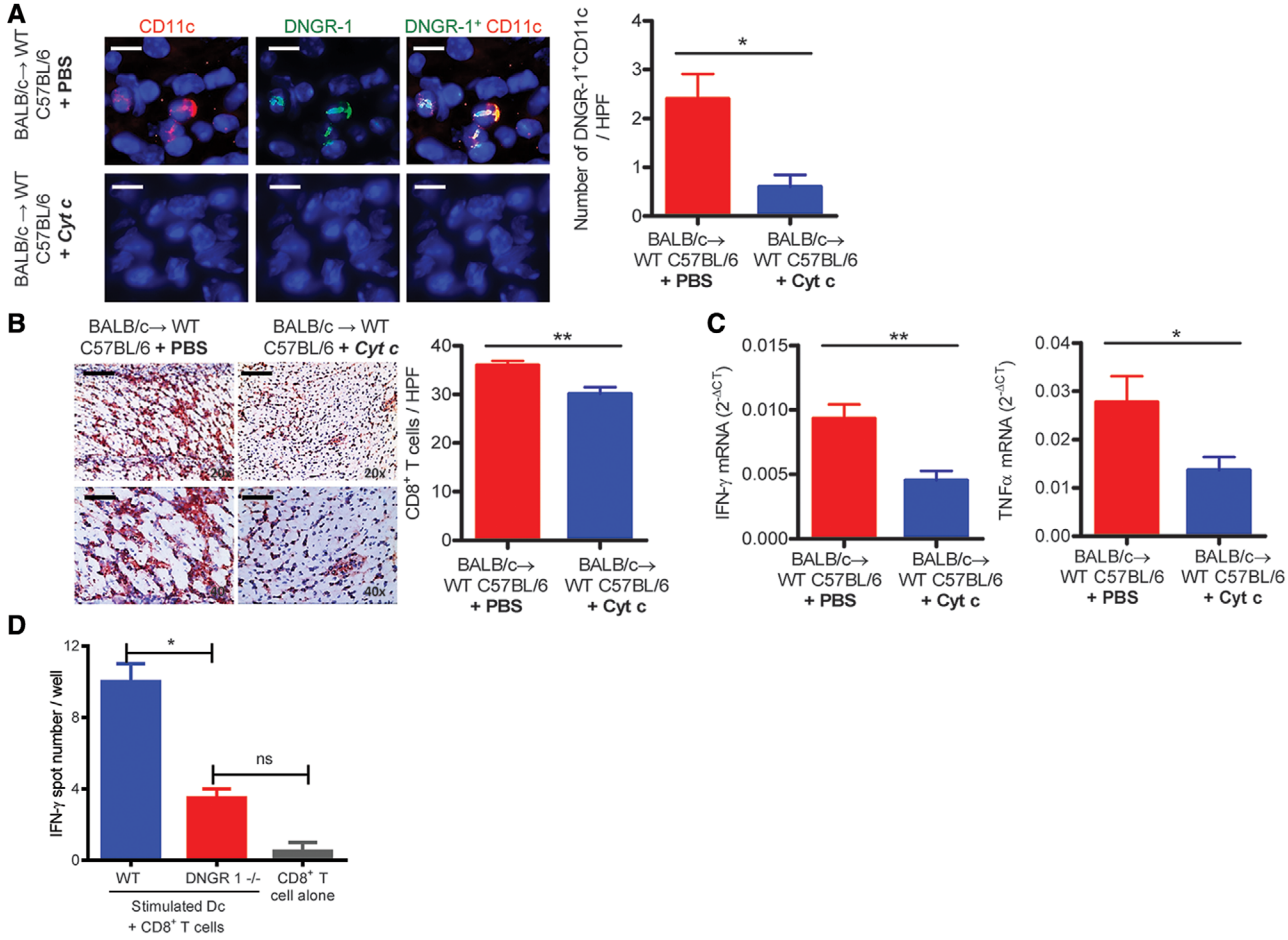

Figure 6. Selective apoptosis and DNGR1$^{-/-}$ in cross-presenting cDC1s reduces indirect CD8$^+$ T cell allorecognition and effector cytokine production. Wild-type C57BL/6 depleted of CD4$^+$ T cells and treated with cytochrome C (Cyt C) (5 mg/mouse in PBS) on days -1, 2, and 7 relative to the day of transplantation (day 0), were transplanted with BALB/c donor hearts (BALB/c → WT C57BL/6 + Cyt C) and analyzed on day 20 after transplantation ($n = 5$ per group). Allogeneic groups with BALB/c → WT C57BL/6 + PBS were used as control. **(A)** Representative IF-staining of DNGR-1$^+$ DC (DNGR-1$^+$ CD11c$^+$ in yellow, the nucleus is stained in blue) and their quantification (DNGR-1$^+$ DC/total CD11c positive cells (in red) per HPF within the allografts of Cyt C treated compared to PBS control groups is depicted. Scale bar 50 μm, magnification 40×. **(B)** Immunohistochemical staining showing CD8$^+$ T cells (positive cells are in brown) and their quantification per HPF within the Cyt C compared to PBS-treated allogeneic transplants. Scale bar 100 μm in 20× magnification and Scale bar 50 μm in 40× magnification. **(C)** Determination of mRNA expression (normalized against housekeeping gene β-actin) of CD8 T effector cytokines IFN-γ and TNF-α within the allografts of Cyt C treated recipients compared to PBS control groups. **(D)** Indirect pathway IFN-γ Elispot: CD11c$^+$ cells were isolated from spleens of WT and DNGR-1$^{-/-}$ C57BL/6 recipient mice and loaded with alloantigen from allografts (BALB/c→C57BL/6, day 5 post transplantation). Splenic C57BL/6 CD8$^+$ T cells were co-incubated for 3 days. Number of spots (IFN-γ expressing cells) per well are compared between WT and DNGR-1$^{-/-}$ group. WT alone group (only C57BL/6 CD8$^+$ T cells) was used as negative control. (A–D) Data are from two independent experiments and are shown as mean ± SD and Mann–Whitney *U*-test was applied to compare two groups. $^*p \le 0.05$; $^{**}p \le 0.01$.

induction of rejection-associated cytokines (IFN-γ $p = 0.0002$, IL-33 $p = 0.0393$; Fig. 7E).

We corroborated these results in the fully immunocompetent Bm12→C57BL/6 heart transplantation model. In this model, temporary CD4$^+$ T cell depletion is not necessary to induce chronic allograft rejection and fibrotic organ remodeling. Antibody blockade of DNGR-1 also resulted in reduction of chronic rejection and fibrosis, similar to the extent seen in the BALB/c into C57BL/6 with CD4$^+$ T cell depletion model (Supporting Information Fig. S7A–E). Therefore, DNGR-1 blockade is a useful means of ameliorating chronic rejection in two mouse models of allotransplantation.

Discussion

A transplanted organ experiences various traumas, from physical manipulation to varying oxygen tension, that can cause death of graft cells and consequently cause release of DAMPs [15,44]. DAMPs have been proposed to contribute to the inordinate immunogenicity of allografts through engagement of DAMP receptors on host immune cells but the mechanisms involved remain unclear [12,15]. Here, we establish a connection between DAMP recognition and chronic CD8$^+$ T cell-mediated responses leading to cardiac allograft fibrosis. We show that a subset of specialized DCs with a superior capacity to cross-prime CD8$^+$ T cells,

© 2020 The Authors. *European Journal of Immunology* published by WILEY-VCH Verlag GmbH & Co. KGaA, Weinheim.

15214141, 2020, 12, Downloaded from https://onlinelibrary.wiley.com/doi/10.1002/eji.201948501 by Open Access University of Augsburg - Universitätsbibliothek Augsburg , Wiley Online Library on [04/05/2026]. See the Terms and Conditions (https://onlinelibrary.wiley.com/terms-and-conditions) on Wiley Online Library for rules of use; OA articles are governed by the applicable Creative Commons License

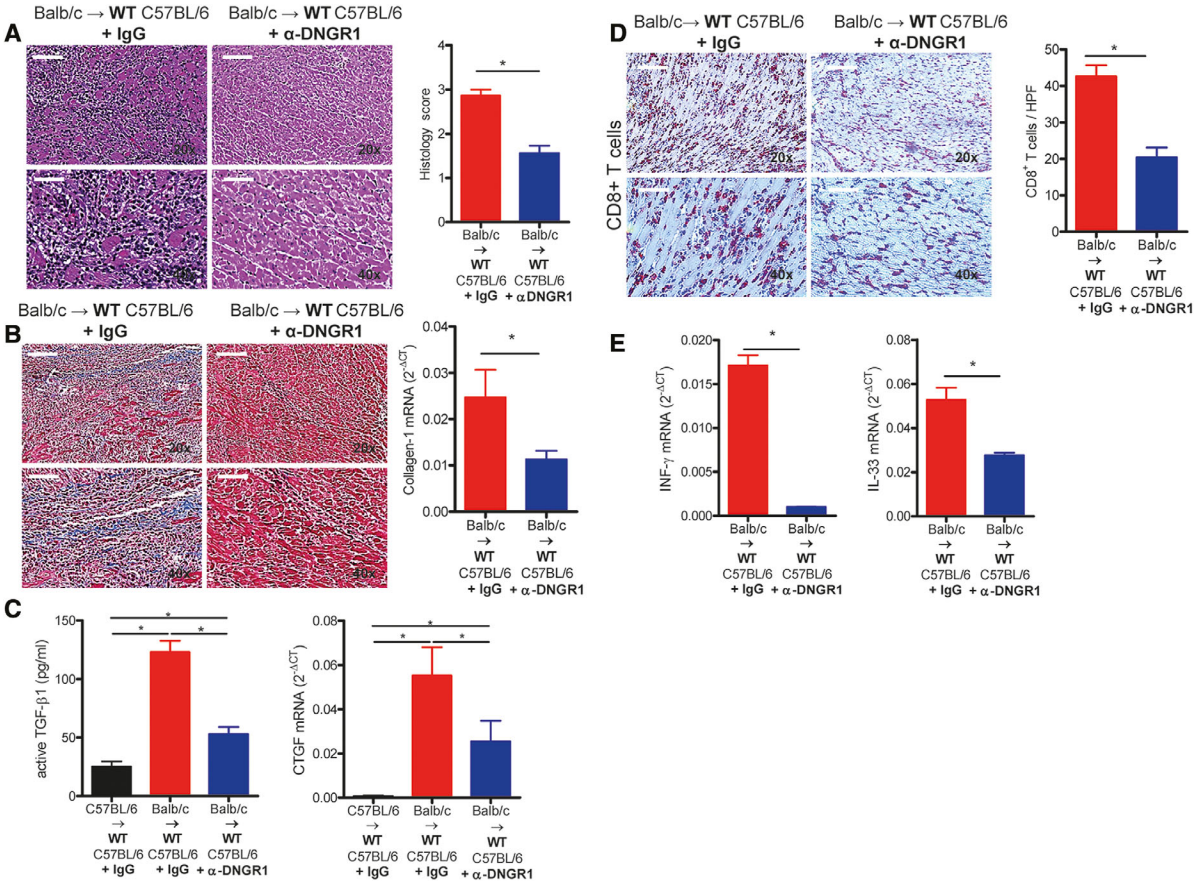

Figure 7. Blockade of DNGR-1 prevents fibrosis and chronic cardiac allograft rejection in BALB/c → C57BL/6 model. Wild-type C57BL/6 depleted of $CD4^+$ T cells and treated with anti-DNGR-1 monoclonal antibody, mAb (100 μg i.p. in PBS), or IgG1 as control, on days 0, 3, 10, and 17 relative to the day of transplantation (day 0) were transplanted with BALB/c donor hearts (BALB/c → WT C57BL/6 + α-DNGR-1) and analyzed on day 20 ($n = 5$ per group). Allogeneic groups with BALB/c → WT C57BL/6 + IgG were used as control. (**A**) Representative H&E-staining of cell infiltration and histology score (graph on the right) of the allografts transplanted into anti-DNGR-1-treated recipients compared to the isotype control groups are illustrated. Scale bar 100 μm in 20× magnification and Scale bar 50 μm in 40× magnification. (**B**) Representative MT-staining of collagen deposition (in blue) and quantification of mRNA expression (normalized against housekeeping gene β-actin) of collagen (graph) within the allografts transplanted into anti-DNGR-1-treated recipient compared to the group that received IgG are shown. Scale bar 100 μm in 20× magnification and Scale bar 50 μm in 40× magnification. (**C**) Quantification of active TGF-β_1 and mRNA expression of CTGF within the allografts transplanted into anti-DNGR-1-treated recipients compared to the IgG groups. (**D**) Immunohistochemical staining showing $CD8^+$ T cells (positive cells are in brown) and their quantification per HPF (graph) within the anti-DNGR-1 treated compared to isotype treated allogeneic transplants. Scale bar 100 μm in 20× magnification and Scale bar 50 μm in 40× magnification. (**E**) Determination of mRNA (normalized against housekeeping gene β-actin) expression of effector cytokine (IFN-γ and IL-33) within the allografts transplanted into anti-DNGR-1 treated recipient compared to control group that received IgG. (A–E) Data are from two independent experiments and are shown as mean ± SD and Mann–Whitney *U*-test was applied to compare two groups. $^*p \leq 0.05$.

cDC1s, is absolutely crucial for $CD8^+$ T cell-mediated allograft rejection. Importantly, we further reveal a critical role for the DAMP receptor, DNGR-1, expressed by the cDC1 subset in mediating this rejection and show that blockade of this receptor contributes to allograft acceptance. Our findings help illuminate the immune mechanisms involved in allograft rejection and highlight how increased understanding of such processes can suggest potential avenues for therapeutic intervention.

Allograft rejection is the result of a complex interplay of mechanisms and factors [5]. Rejection episodes are mainly driven by $CD4^+$ Th1 cells that produce IFN-γ and TNF [45,46]. In the absence of a Th1-mediated alloimmune responses, $CD4^+$ Th17 cells can also drive a pro-inflammatory response that accelerates chronic allograft rejection with IL-17A as a key cytokine [47]. In this study, we utilized depletion of $CD4^+$ cells to reveal an important yet underappreciated role also for $CD8^+$ T cells in the development of chronic organ rejection [48–50]. The fact that $CD8^+$ T cells can contribute to such rejection highlights their importance as potential targets in immunotherapies aimed at provoking long-term graft acceptance.

The most straightforward interpretation of our experiments is that DNGR-1^+ cDC1s infiltrate allogeneic grafts and acquire allograft antigens. Some of those cDC1 then migrate to draining lymph nodes where they cross-present the graft antigens on MHC class I and cross-prime $CD8^+$ T cells. The primed T cells can then home to the graft and produce effector cytokines such as IFN-γ and IL-33. As a consequence, active TGF-β_1 and CTGF are induced locally and lead to allograft fibrosis. The conundrum is that,

© 2020 The Authors. *European Journal of Immunology* published by WILEY-VCH Verlag GmbH & Co. KGaA, Weinheim.

15214141, 2020, 12, Downloaded from https://onlinelibrary.wiley.com/doi/10.1002/eji.201948501 by Open Access University of Augsburg - Universitätsbibliothek Augsburg , Wiley Online Library on [04/05/2026]. See the Terms and Conditions (https://onlinelibrary.wiley.com/terms-and-conditions) on Wiley Online Library for rules of use; OA articles are governed by the applicable Creative Commons License

leaving aside the possibility of cross-dressing [51], the primed $CD8^+$ T cells are restricted by host MHC and, therefore, cannot be restimulated directly by allograft cells. It is possible, therefore, that they are restimulated within the graft once again by cDC1 locally cross-presenting alloantigens, which would reinforce the observed dependence on that DC subtype and on the DNGR-1 receptor. An analogous role for cDC1 has been proposed in tumor immunity whereby cDC1 prime an antitumor $CD8^+$ T cell response in tumor draining lymph nodes but also restimulate effector $CD8^+$ T cells within the tumor itself [52–54]. The fact that $CD8^+$ T cells would utilize the indirect presentation pathway to respond to alloantigens within grafts may also explain why their primary contribution in this setting appears to be production of cytokines leading to fibrosis rather than direct acute destruction of allograft cell targets as the latter cannot be directly recognized.

DAMP release and inflammation due to transplantation should be the same in syn- and allografts yet, in our study, cDC1 accumulated to a much greater extent in allografts than in syngeneic grafts. One point that remains unclear is why and how allogeneity is detected at these early time points to control accumulation of cDC1s. Early accumulation of alloreactive T-cells could be involved and those cells could produce chemokines such as XCL1/2 that attract cDC1 in a positive feedback cycle [55,56]. However, we saw no difference in cDC1 accumulation in allografts transplanted into mice lacking $CD8^+$ T cells (data not shown). Alternatively, allogeneic determinants might be recognized early after transplantation not by T cells but by host NK cells that produce XCL1/2 and CCL5 to recruit cDC1 into grafts as recently demonstrated for tumors [57]. Further experimentation will be necessary to assess these possibilities.

In summary, our experiments suggest that immune activation leading to chronic allograft rejection and fibrosis can be triggered by DAMPs, including F-actin, that are detected by graft-infiltrating host cells. F-actin is recognized by DNGR-1, a receptor that is expressed on cDC1s that develop under the control of the transcription factor Batf3. DNGR-1 is a universal marker of mouse and human cDC1s in lymphoid and non-lymphoid tissues [18–22,24] and targeting antigens to DNGR-1 receptor has been used to induce specific immune responses in vaccination modalities [18,58,59]. In this current study, antibodies to DNGR-1 were used instead to block the receptor and shown to be effective at preventing chronic graft rejection in two different mouse heart transplantation model. These experiments suggest that antibody blockade of DNGR-1 can prevent the immune cascade leading to chronic allograft rejection and fibrosis and could therefore be exploited in humans in a therapeutic setting.

Materials and methods

Mice

Eight to 10 weeks (w) old female BALB/c ($H\text{-}2^d$) and Bm12 ($H2\text{-}Ab1^{bm12}$) as donors and 12–14 weeks old WT and deficient (-/-) *Batf3*$^{tm1Kmm/J}$ ($Batf3^{-/-}$) and Clec9a$^{tm1.1Crs/J}$ ($Clec9a^{-/-}$) recipient female mice on C57BL/6 ($H\text{-}2^b$) background were purchased from Jackson Laboratory (Bar Harbor ME, USA). Mice were then bred in the animal facility of the Department of Surgery (University Medical Center Regensburg, Germany). All mice were housed under pathogen-free conditions and handled according to the local institutional guidelines. The experiments were approved by the local animal committee (TVA DMS-2532-2-102).

Heterotopic heart transplantation

Cardiac allografts from donors BALB/c and Bm12 mice were heterotopically transplanted into WT and $C57BL/6^{-/-}$ as previously established by Corry et al. and adapted in our laboratory [2,5,60,48]. Donor hearts were perfused through the abdominal vena cava with 3 mL of cold 0.9% saline containing 500 IE heparin (Ratiopharm, Ulm, Germany) then harvested and placed in 4°C saline until transplantation. Abdominal palpation was regularly carried out to ensure the beating of the allograft. Functioning hearts were then harvested for analyses. In the BALB/c→C57BL/6 model transient $CD4^+$ T cell-depletion was used for generation of chronic allograft rejection [48–50]. This model further allows investigation of allograft rejection in absence of $CD4^+$ T cells. The Bm12→C57BL/6 model is a fully immunocompetent model also with the development of chronic allograft rejection.

Human samples

Chronic rejected and control human cardiac graft specimens were obtained from surgical biopsies (Department of Cardiac Surgery, Bad Oeynhausen, Germany). The paraffin-embedded tissue samples were sectioned at 3–4 μm. This was approved by the local ethics committee.

Antibody treatment

$CD4^+$ T cell depletion in vivo: Recipient mice were injected intraperitoneally (i.p.; 1 mg/mouse) on day -1, 0, and 7 relative to day of transplantation (day 0) with rat anti-mouse CD4 monoclonal antibody, mAb (IgG2b, clone GK 1.5; Bioxcell, Cologne, Germany) to transiently deplete $CD4^+$ T cells as previously described [61].

DNGR-1 antibody blocking in vivo: Rat anti-mouse DNGR-1 (7H11) mAb has been described [18, 27]. Recipient mice received 100 μg of mAb i.p. in PBS or, as control, only PBS on day 0, 3, 10, and 17 after transplantation.

Cytochrome C depletion in vivo: Cytochrome C (Cyt C) is known to be able to induce an Apaf-1-dependent apoptosis selectively in cross-presenting DCs (https://doi.org/10.1073/pnas.0712394105). Horse heart Cyt C (C2506, Sigma, St. Louis, MO) was dissolved in PBS at 20–50 mg/mL ant stocked at -20°C. All treatments of recipient mice were performed in vivo

© 2020 The Authors. *European Journal of Immunology* published by WILEY-VCH Verlag GmbH & Co. KGaA, Weinheim.

15214141, 2020, 12, Downloaded from https://onlinelibrary.wiley.com/doi/10.1002/eji.201948501 by Open Access University of Augsburg - Universitätsbibliothek Augsburg , Wiley Online Library on [04/05/2026]. See the Terms and Conditions (https://onlinelibrary.wiley.com/terms-and-conditions) on Wiley Online Library for rules of use; OA articles are governed by the applicable Creative Commons License

15214141, 2020, 12, Downloaded from https://onlinelibrary.wiley.com/doi/10.1002/eji.201948501 by Open Access University of Augsburg - Universitätsbibliothek Augsburg , Wiley Online Library on [04/05/2026]. See the Terms and Conditions (https://onlinelibrary.wiley.com/terms-and-conditions) on Wiley Online Library for rules of use; OA articles are governed by the applicable Creative Commons License

and consisted of 5 mg doses of Cyt C in PBS administered intravenously (i.v.) on day 1 prior heart transplantation then subcutaneously (s.c.) on day 2 and 7 post heart transplantation. Recipient receiving only PBS solution (100 μL/mouse) were used as control groups.

Cardiac cell isolation

Cells were isolated from cardiac grafts as previously described [48]. Briefly, tissue was minced with scalpels in the presence of sterile RPMI 1640 medium containing 10% FCS, 600 U/ml collagenase II (Roche Diagnostics, Mannheim, Germany) and deoxyribonuclease I (DNAse, from bovine pancreas; Sigma, Munich, Germany). The mixture was slowly shaken at room temperature (RT) for 2 h. The supernatant (SN) was obtained and filtered through a 100-μm-nylon cell strainer. Remaining tissue was again digested in 5 mL of same solution at 37°C and then strained. Filtered material was centrifuged and red blood cells were lysed with ACK lysis buffer (BioWhittacker, Lonza, MD, USA). The pellet containing cells was passed through a 40-μm-nylon cell strainer. For the $CD8^+$ T cell isolation, negative selection procedure was performed as recommended by manufacturer (MACS, Miltenyi Biotec: mouse $CD8a^+$ T Cell Isolation Kit). After elution of MicroBeads conjugated cells through magnetic MACS LS column, the fraction containing $CD8^+$ T cells was recovered and washed by centrifugation.

Histology and immunohistochemistry

Formalin-fixed and paraffin-embedded (mouse and human) or frozen (mouse) cardiac graft specimens were prepared and sectioned (3–4 μm). For hematoxylin and eosin staining, paraffin-embedded sections were deparaffinized and fixed successively in Roti and ethanol solutions. Slides were washed with water and stained in hematoxylin for 13 s, washed again, and immersed in eosin for 2–4 min. Slides were returned with washing to the fixation buffers beginning from ethanol to roti and mounted with Roti®-Histokitt mounting medium (Carl Roth GmbH + Co. KG, Karlsruhe, Germany) for microscopy. For immunohistochemistry (IHC), after deparaffinization and fixation (immersion into Roti and ethanol for paraffin-embedded and in methanol-ethanol solution for frozen sections), slides were blocked with PBS+20% goat serum (Sigma–Aldrich, St Louis, MO, USA) for 20 min at RT. After incubation overnight (O/N) in humid chamber at 4°C, slides were stained with monoclonal rat anti-mouse CD8a antibody (Ab25478; Abcam, Cambridge, UK; dilution 1:50) in PBS + 1% goat serum (GS). After washing with PBS, slides were stained with the secondary goat anti-rat-Fab2 (sc-3822; Santa Cruz Biotechnology, Heidelberg, Germany) for 1 h at RT in PBS+ 1% GS. Then, sections were incubated with SensiTek HRP solution (ScyTec Laboratories, Logan, UT, USA) and positive signals were visualized using an AEC+ High Sensitivity Substrate Chromogen kit (Dako, Hamburg, Germany). Slides were finally mounted using Aquatex® aqueous mounting agent (Merck KGaA, Darmstadt, Germany) and images were taken with Axio Observer Z1 microscope (Carl Zeiss, Oberkochen, Germany). For the evaluation of cardiac allograft rejection, the revised 2004 ISHLT grading system was used [23]. Graft-infiltrating $CD8^+$ cells were manually counted using ImageJ software version 1.48 (http://imagej.nih.gov/ij), in ten high power fields (HPFs) at 20× magnification. For analysis, at least 10 high-power fields (HPF) were selected per slide. All results are presented as the mean ± SEM and all analysis was performed in a blinded fashion.

Immunofluorescence

Slides were stained as described in immunohistochemistry section until primary Ab step. The primary antibodies: Armenian Hamster monoclonal antibody (ab119342: Abcam, Cambridge, UK) against CD11c (mouse and human), Rat purified IgG1 (BioLegend, Fell, Germany) against DNGR-1 (mouse), Mouse purified IgG1 (BioLegend) against DNGR-1 (human), and rabbit monoclonal antibody (ab52903) against phosphorolysed Smads3, Phospho-Smad3 (mouse and human) were used (at dilution 1:50 in PBS+ 1% goat serum) and samples were incubated O/N at 4°C. Secondary (Cy2 or Cy3) conjugated goat anti-rabbit, goat anti-rat, goat ant-mouse, or goat anti-Armenian Hamster IgG were used for detection. For the H-2b and H-2d positive cells detection, primary antibodies PE-conjugated anti-mouse H-2b (eBioscience, clone: AF6-88-5.5.3) and anti-mouse H-2d (BioLegend, clone: SF1-1.1) were used at dilution 1:150. Polyclonal rabbit anti-PE (Novus Biologicals) as secondary antibody was used at dilution 1:150, then Cy5 conjugated goat anti-rabbit (Dianova) was used for the detection. DNA was labelled with 4',6-Diamidino-2-Phenylindole, Dihydrochloride (DAPI; dilution 1:2000-5000 in PBS+1% goat serum) for 2–3 min. Reaction was stopped using distilled water and slides were mounted with Fluorescence Mounting Medium (Dako, Hamburg, Germany). Images were taken using an Axio Visio microscope (Carl Zeiss, Oberkochen, Germany). For the analysis, at least 10 high-power fields were selected per slide in a blinded fashion.

Masson's trichrome staining

Formalin-fixed and paraffin-embedded graft tissue samples (mouse and human) were deparaffinized and fixed as described above in H&E staining. To improve staining quality, sections were fixed in a Bouin's solution (Sigma–Aldrich) for 30 min at 56°C. Successively, slides were stained for 10–15 min in Weigert's iron hematoxylin working solution, Biebrich scarlet-acid fuchsin and differentiated in phosphomolybdic-phosphotungstic acid solution (Sigma–Aldrich) for each solution. Then, slides were transferred into aniline blue solution (Sigma–Aldrich) and briefly differentiated in 1% acetic acid. After returning to the ethanol and Roti solution, slides were mounted with Roti®-Histokitt mounting medium and observed using Axio Visio microscope.

© 2020 The Authors. *European Journal of Immunology* published by WILEY-VCH Verlag GmbH & Co. KGaA, Weinheim.

Flow cytometry (FACS)

After collagenase digestion of harvested grafts and production of a single-cell solution graft-infiltrating cells were stained using fluorochrome-conjugated mouse-specific antibodies (all Abs were from eBioscience, Frankfurt, Germany). Data were acquired using a FACS Canto II flow cytometer (BD, Heidelberg, Germany) and analyzed using FlowJo software (version 8.8.6) in adherence to Guidelines for the use of flow cytometry and cell sorting in immunological studies [62]

RNA isolation, RT-PCR, and PCR array

Total RNA was extracted from whole allografts or isolated $CD8^+$ T cells using the RNeasy Mini Kit (Qiagen, Hilden, Germany) according to the manufacturer's instructions. One microgram of total RNA was reverse transcribed using the AffinityScriptTM QPCR cDNA Synthesis Kit (Aiglent Technologies, Böblingen, Germany). Quantitative Real-time PCR (qRT-PCR) assay was performed to quantify collagen 1, CTGF, TGF-β1, IFN-γ, and IL-33 expression using the QuantiTect SYBR Green PCR Kit (Qiagen GmbH, Hilden, Germany) and the Roche LightCycler480 System. The following primer sequences were used: forward (sense) 5'-TGTTCAGCTTTGTGGACCTC-3', reverse (anti-sense) 5'-TCAAGCATACCTCGGGTTTC-3' (mouse collagen, procollagen 1a); forward 5' AGAGGGAAATCGTGCGTGAC-3', reverse 5'-CAATAGTGATGACCTGGCCGT-3' (mouse β-actin); forward 5'-TTGCTTCAGCTCCACAGAGA-3', reverse 3' TGGTTGTAGAGGGCAAGGAC-5' (mouse TGF-β1); forward 5'-GGAAAACATTAAGAAGGGAAAA-3', reverse 3'-CCGCAGAACTTAGCCCTGTA-5 (mouse CTGF); Forward 5′-ACTGGCAAAGGATGGTGAC-3′, Reverse 3′-CTCCAGTTGTTGGGTGTCCA-5′ mouse IFN-γ); and Forward 5' CACATTGAGCATCCAAGGAA-3', Reverse 5' AACAGATTGGTCATTGTATGTACTCAG-3' (mouse IL-33). Relative gene expression was determined using the $2^{-\Delta CT}$ method (normalized to the mean of the expression level for the housekeeper β-actin). Mouse Necrosis/apoptosis related-gene expression was evaluated using a mouse Necrosis RT^2 Profiler PCR Array kit (SA Biosciences, Hilden, Germany) using LightCycler 480 Real-Time PCR System (Roche). Mean of triplicated well values and fold change in expression relative to control were considered for each sample.

Indirect pathway IFN-γ-Elispot

WT and $Clec9a^{-/-}$ recipient's APCs were isolated using mouse CD11c MicroBeads UltraPure isolation kit (Miltenyi Biotec, Bergisch Gladbach, Germany) and loaded for 3 day in cultures with 500 μg/mL of alloantigen. Alloantigen (protein lysate) was isolated after sonication in PBS 1× solution of allografts (Balb/c→C57BL/6) harvested on day 5 after heart transplantation. Protein concentration in the lysate was measured using Bradford protein assay (B6916, Sigma-Aldrich). Note that 200 μL/well of culture medium containing 300 000 of $CD11c^+$ DCs and 500 μg/mL of alloantigen was added and incubated for 3 days at 37°C and 5% CO_2. Then, splenic C57BL/6 WT $CD8^+$ T cells were isolated using mouse $CD8a^+$ T cell isolation Kit (Miltenyi Biotec). Elispot was performed using a MB Multiscreen PVDF plate (MAIPS4510, Millipore). Plates were pre-coated with an IFN-γ antibody (3321-2A, Mabtech) for 2 h at 37°C and 5% CO_2. Antigen-loaded DCs (as stimulators) were added to the plates with splenic C57BL/6 WT $CD8^+$ T cells (as effectors) at a ratio of 50 000:150 000 and incubated for 3 days at 37°C and 5% CO_2. Following removal of the cells and washing of the plate wells, biotinylated specific detection antibodies (3321-2A, R4-6A2, Mabtech) were added to the wells. The resulting antibody complex was thus detected by addition of Streptavidin-ALP-labeled conjugate (3321-2A, Mabtech) and 1-Step NBT/BCIP substrate solution (34042, ThermoFisher Scientific). Spots were counted with a specific Elispot reader (EliSpot Robotic System ELROB05i, AID Advanced Imaging Devices GmbH Straßberg).

Statistics

All groups are shown as mean ± SD of the mean and were compared using a one-tailed Student's *t*-test or Mann–Whitney *U*-test (GraphPad Prism, version 5.00). The log-rank test was used to compare graft survival between the groups. Difference among groups was considered statistically significant (*) if p was < 0.05.

Acknowledgments: This work was supported by the University of Regensburg (Reform A; Stefan M. Brunner). Work in the CRS laboratory was supported by The Francis Crick Institute, which receives core funding from Cancer Research UK (FC001136), the UK Medical Research Council (FC001136), and the Wellcome Trust (FC001136), and by an ERC Advanced Investigator grant (AdG 786674), a Wellcome Investigator Award (WT106973MA) and a prize from The Louis-Jeantet Foundation (Caetano Reis e Sousa).
Open access funding enabled and organized by Projekt DEAL.

Conflict of interest: The authors of this manuscript have no commercial or financial conflicts of interest.

References

1 **Racusen, L. C., Solez, K.** and **Colvin, R.**, Fibrosis and atrophy in the renal allograft: interim report and new directions. *Am. J. Transplant.* 2002. **2**: 203–206.

© 2020 The Authors. *European Journal of Immunology* published by WILEY-VCH Verlag GmbH & Co. KGaA, Weinheim.

15214141, 2020, 12, Downloaded from https://onlinelibrary.wiley.com/doi/10.1002/eji.201948501 by Open Access University of Augsburg - Universitätsbibliothek Augsburg , Wiley Online Library on [04/05/2026]. See the Terms and Conditions (https://onlinelibrary.wiley.com/terms-and-conditions) on Wiley Online Library for rules of use; OA articles are governed by the applicable Creative Commons License

2 **Brunner, S. M.**, **Schiechl, G.**, **Kesselring, R.**, **Martin, M.**, **Balam, S.**, **Schlitt, H. J.**, **Geissler, E. K.** et al., IL-13 signaling via IL-13Ralpha2 triggers TGF-beta1-dependent allograft fibrosis. *Transplant. Res.* 2013. **2**: 16.

3 **Pichler, M.**, **Rainer, P. P.**, **Schauer, S.** and **Hoefler G.**, Cardiac fibrosis in human transplanted hearts is mainly driven by cells of intracardiac origin. *J. Am. Coll. Cardiol.* 2012. **59**: 1008–1016.

4 **Huibers, M.**, **De Jonge, N.**, **Van Kuik, J.**, **Siera-De Koning, E.**, **Van Wichen, D.**, **Dullens, H.**, **Schipper, M.** et al., Intimal fibrosis in human cardiac allograft vasculopathy. *Transpl. Immunol.* 2011. **25**: 124–132.

5 **Brunner, S. M.**, **Schiechl, G.**, **Falk, W.**, **Schlitt, H. J.**, **Geissler, E. K.** and **Fichtner-Feigl, S.**, Interleukin-33 prolongs allograft survival during chronic cardiac rejection. *Transpl. Int.* 2011. **24**: 1027–1039.

6 **Battaglia, M.**, Potential T regulatory cell therapy in transplantation: how far have we come and how far can we go? *Transpl. Int.* 2010. **23**: 761–770.

7 **Wang, H.**, **Hosiawa, K. A.**, **Min, W.**, **Yang, J.**, **Zhang, X.**, **Garcia, B.**, **Ichim, T. E.** et al., Cytokines regulate the pattern of rejection and susceptibility to cyclosporine therapy in different mouse recipient strains after cardiac allografting. *J. Immunol.* 2003. **171**: 3823–3836.

8 **Bueno, V. P.J.**, The role of CD8+ T cells during allograft rejection. *Braz. J. Med. Biol. Res.* 2002. **35**: 1247–1258.

9 **Youssef, A. R.**, **Otley, C.**, **Mathieson, P. W.** and **Smith, R. M.**, Role of CD4+ and CD8+ T cells in murine skin and heart allograft rejection across different antigenic desparities. *Transpl Immunol* 2004. **13**: 297–304.

10 **Seong, S. Y.** and **Matzinger, P.**, Hydrophobicity: an ancient damage-associated molecular pattern that initiates innate immune responses. *Nat. Rev. Immunol.* 2004. **4**: 469–478.

11 **Brown, G. D.**, Immunology: Actin' dangerously. *Nature* 2012. **485**: 589–590.

12 **Matzinger, P.**, The danger model: a renewed sense of self. *Science* 2002. **296**: 301–305.

13 **Land, W.**, **Schneeberger, H.**, **Schleibner, S.**, **Illner, W. D.**, **Abendroth, D.**, **Rutili, G.**, **Arfors, K. E.** et al., The beneficial effect of human recombinant superoxide dismutase on acute and chronic rejection events in recipients of cadaveric renal transplants. *Transplantation* 1994. **57**: 211–217.

14 **Zelenay, S.** and **Reis e Sousa, C.**, Adaptive immunity after cell death. *Trends Immunol.* 2013. **34**: 329–335.

15 **Land, W. G.**, Emerging role of innate immunity in organ transplantation part III: the quest for transplant tolerance via prevention of oxidative allograft injury and its consequences. *Transplant Rev (Orlando)* 2012. **26**: 88–102.

16 **Ahrens, S.**, **Zelenay, S.**, **Sancho, D.**, **Hanč, P.**, **Kjær, S.**, **Feest, C.**, **Fletcher, G.** et al., F-actin is an evolutionarily conserved damage-associated molecular pattern recognized by DNGR-1, a receptor for dead cells. *Immunity.* 2012. **36**: 635–645.

17 **Hanc, P.**, **Fujii, T.**, **Iborra, S.**, **Yamada, Y.**, **Huotari, J.**, **Schulz, O.**, **Ahrens, S.** et al., Structure of the Complex of F-Actin and DNGR-1, a C-Type Lectin Receptor Involved in Dendritic Cell Cross-Presentation of Dead Cell-Associated Antigens. *Immunity.* 2015. **42**: 839–849.

18 **Sancho, D.**, **Mourão-Sá, D.**, **Joffre, O. P.**, **Schulz, O.**, **Rogers, N. C.**, **Pennington, D. J.**, **Carlyle, J. R.** et al., Tumor therapy in mice via antigen targeting to a novel, DC-restricted C-type lectin. *J. Clin. Invest.* 2008. **118**: 2098–2110.

19 **Huysamen, C.**, **Willment, J. A.**, **Dennehy, K. M.** and **Brown, G. D.**, CLEC9A Is a Novel Activation C-type Lectin-like Receptor Expressed on BDCA3+ Dendritic Cells and a Subset of Monocytes. *J. Biol. Chem.* 2008. **283**: 16693–16701.

20 **Schraml, B. U.**, **van Blijswijk, J.**, **Zelenay, S.**, **Whitney, P. G.**, **Filby, A.**, **Acton, S. E.**, **Rogers, N. C.** et al., Reis e Sousa C. Genetic tracing via DNGR-1 expression history defines dendritic cells as a hematopoietic lineage. *Cell* 2013. **154**: 843–858.

21 **Murphy, T. L.**, **Tussiwand, R.** and **Murphy, K. M.**, Specificity through cooperation: BATF–IRF interactions control immune-regulatory networks. *Nat. Rev. Immunol.* 2013. **13**: 499–509.

22 **Edelson, B. T.**, **KC, W.**, **Juang, R**, **Kohyama, M.**, **Benoit, L. A.**, **Klekotka, P. A.**, **Moon, C.** et al., Peripheral CD103+ dendritic cells form a unified subset developmentally related to CD8alpha+ conventional dendritic cells. *J. Exp. Med.* 2010. **207**: 823–836.

23 **Hasegawa, T.**, **Visovatti, S. H.**, **Hyman, M. C.**, **Hayasaki, T.** and **Pinsky, D. J.**, Heterotopic vascularized murine cardiac transplantation to study graft arteriopathy. *Nat. Protoc.* 2007. **2**: 471–480.

24 **Poulin, L. F.**, **Reyal, Y.**, **Uronen-Hansson, H.**, **Schraml, B. U.**, **Sancho, D.**, **Murphy, K. M.**, **Håkansson, U. K.** et al., DNGR-1 is a specific and universal marker of mouse and human Batf3-dependent dendritic cells in lymphoid and nonlymphoid tissues. *Blood* 2012. **119**: 6052–6062.

25 **Hildner, K.**, **Edelson, B. T.**, **Purtha, W. E.**, **Diamond, M.**, **Matsushita, H.**, **Kohyama, M.**, **Calderon, B.** et al., Batf3 deficiency reveals a critical role for CD8alpha+ dendritic cells in cytotoxic T cell immunity. *Science* 2008. **322**: 1097–1100.

26 **Edelson, B. T.**, **Bradstreet, T. R.**, **KC, W.**, **Hildner, K.**, **Herzog, J. W.**, **Sim, J.**, **Russell, J. H.** et al., Batf3-dependent CD11b(low/-) peripheral dendritic cells are GM-CSF-independent and are not required for Th cell priming after subcutaneous immunization. *PLoS One* 2011. **6**: e25660.

27 **Sancho, D.**, **Joffre, O. P.**, **Keller, A. M.**, **Rogers, N. C.**, **Martínez, D.**, **Hernanz-Falcón, P.**, **Rosewell, I.** et al., Identification of a dendritic cell receptor that couples sensing of necrosis to immunity. *Nature* 2009. **458**: 899–903.

28 **Zelenay, S.**, **Keller, A. M.**, **Whitney, P. G.**, **Schraml, B. U.**, **Deddouche, S.**, **Rogers, N. C.**, **Schulz, O.** et al., The dendritic cell receptor DNGR-1 controls endocytic handling of necrotic cell antigens to favor cross-priming of CTLs in virus-infected mice. *J. Clin. Invest.* 2012. **122**: 1615–1627.

29 **Yatim, N.**, **Jusforgues-Saklani, H.**, **Orozco, S.**, **Schulz, O.**, **da Silva, R. B.**, **e Sousa, C. R.**, **Green, D. R.** et al., RIPK1 and NF-kappaB signaling in dying cells determines cross-priming of CD8(+) T cells. *Science* 2015. **350**: 328–334.

30 **Zijlstra, M.**, **Bix, M.**, **Simister, N. E.**, **Loring, J. M.**, **Raulet, D. H.** and **Jaenisch, R.**, Beta 2-microglobulin deficient mice lack CD4-8+ cytolytic T cells. 1990. *J Immunol* 2010. **184**: 4587–4591.

31 **Chefalo, P. J.**, **Grandea, 3rd, A. G.**, **Van Kaer, L.** and **Harding, C. V.**, Tapasin-/- and TAP1-/- macrophages are deficient in vacuolar alternate class I MHC (MHC-I) processing due to decreased MHC-I stability at phagolysosomal pH. *J. Immunol.* 2003. **170**: 5825–5833.

32 **Ljunggren, H. G.**, **Kaer, L. V.**, **Ashton-Rickardt, P. G.**, **Tonegawa, S.** and **Ploegh, H. L.**, Differential reactivity of residual CD8+ T lymphocytes in TAP1 and beta 2-microglobulin mutant mice. *Eur J Immunol* 1995. **25**: 174–178.

33 **Ljunggren, H. G.**, **Kaer, L. V.**, **Sabatine, M. S.**, **Auchincloss, H., Jr**, **Tonegawa, S.** and **Ploegh, H. L.**, MHC class I expression and CD8+ T cell development in TAP1/beta 2-microglobulin double mutant mice. *Int. Immunol.* 1995. **7**: 975–984.

34 **Van Kaer, L.**, **Ashton-Rickardt, P. G.**, **Ploegh, H. L.** and **Tonegawa, S.**, TAP1 mutant mice are deficient in antigen presentation, surface class I molecules, and CD4-8+ T cells. *Cell* 1992. **71**: 1205–1214.

35 **Ardeniz, O.**, **Unger, S.**, **Onay, H.**, **Ammann, S.**, **Keck, C.**, **Cianga, C.**, **Gerçeker, B.** et al., beta2-Microglobulin deficiency causes a complex immunodeficiency of the innate and adaptive immune system. *J. Allergy Clin. Immunol.* 2015. **136**: 392–401.

36 **Hein, Z.**, **Uchtenhagen, H.**, **Abualrous, E. T.**, **Saini, S. K.**, **Janßen, L.**, **Van Hateren, A.**, **Wiek, C.** et al., Peptide-independent stabilization of MHC

© 2020 The Authors. *European Journal of Immunology* published by WILEY-VCH Verlag GmbH & Co. KGaA, Weinheim.

15214141, 2020, 12, Downloaded from https://onlinelibrary.wiley.com/doi/10.1002/eji.201948501 by Open Access University of Augsburg - Universitätsbibliothek Augsburg , Wiley Online Library on [04/05/2026]. See the Terms and Conditions (https://onlinelibrary.wiley.com/terms-and-conditions) on Wiley Online Library for rules of use; OA articles are governed by the applicable Creative Commons License

class I molecules breaches cellular quality control. *J. Cell Sci.* 2014;**127**(Pt 13):2885–2897.

37 **Kamei, H.**, **Masuda, S.**, **Nakamura, T.**, **Oike, F.**, **Takada, Y.**, **Hamajima, N.**, Association of transporter associated with antigen processing (TAP) gene polymorphisms in donors with acute cellular rejection in living donor liver transplantation. *J. Gastrointestin Liver Dis.* 2013. **22**: 167–171.

38 **,Hashmi S.** and **Al-Salam, S.**, Acute myocardial infarction and myocardial ischemia-reperfusion injury: a comparison. *Int. J. Clin. Exp. Pathol.* 2015. **8**: 8786–8796.

39 **Palandri, A.**, **Salvador, V. R.**, **Wojnacki, J.**, **Vivinetto, A. L.**, **Schnaar, R. L.** and **Lopez, P. H. H.**, Myelin-associated glycoprotein modulates apoptosis of motoneurons during early postnatal development via NgR/p75(NTR) receptor-mediated activation of RhoA signaling pathways. *Cell Death Dis.* 2015. **6**: e1876.

40 **Qiu, X.**, **Klausen, C.**, **Cheng, J. C.** and **Leung, P. C. K.**, CD40 ligand induces RIP1-dependent, necroptosis-like cell death in low-grade serous but not serous borderline ovarian tumor cells. *Cell Death Dis.* 2015. **6**: e1864.

41 **Calmon-Hamaty, F.**, **Audo, R.**, **Combe, B.**, **Morel, J.** and **Hahne, M.**, Targeting the Fas/FasL system in Rheumatoid Arthritis therapy: Promising or risky? *Cytokine* 2015. **75**: 228–233.

42 **Fiers, W.**, **Beyaert, R.**, **Declercq, W.** and **Vandenabeele, P.**, More than one way to die: apoptosis, necrosis and reactive oxygen damage. *Oncogene* 1999. **18**: 7719–7730.

43 **Lin, M. L.**, **Zhan, Y.**, **Proietto, A. I.**, **Prato, S.**, **Wu, L.**, **Heath, W. R.**, **Villadangos, J. A.** et al., Selective suicide of cross-presenting CD8+ dendritic cells by cytochrome c injection shows functional heterogeneity within this subset. *Proceedings of the National Academy of Sciences of the United States of America* 2008. **105**: 3029–3034.

44 **Hu, Q.**, **Wood, C. R.**, **Cimen, S.**, **Venkatachalam, A. B.** and **Alwayn, I. P. J.**, Mitochondrial Damage-Associated Molecular Patterns (MTDs) Are Released during Hepatic Ischemia Reperfusion and Induce Inflammatory Responses. *PLoS One* 2015. **10**: e0140105.

45 **Koglin, J.**, **Glysing-Jensen, T.**, **Gadiraju, S.** and **Russell, M. E.**, Attenuated cardiac allograft vasculopathy in mice with targeted deletion of the transcription factor STAT4. *Circulation* 2000. **101**: 1034–1039.

46 **Liblau, R. S.**, **Singer, S. M.** and **McDevitt, H. O.**, Th1 and Th2 CD4+ T cells in the pathogenesis of organ-specific autoimmune diseases. *Immunol Today* 1995. **16**: 34–38.

47 **Yuan, X.**, **Paez-Cortez, J.**, **Schmitt-Knosalla, I.**, **D'Addio, F.**, **Mfarrej, B.**, **Donnarumma, M.**, **Habicht, A.** et al., A novel role of CD4 Th17 cells in mediating cardiac allograft rejection and vasculopathy. *J. Exp. Med.* 2008. **205**: 3133–3144.

48 **Schiechl, G.**, **Brunner, S. M.**, **Kesselring, R.**, **Martin, M.**, **Ruemmele, P.**, **Mack, M.**, **Hirt, S. W.** et al., Inhibition of innate co-receptor TREM-1 signaling reduces CD4(+) T cell activation and prolongs cardiac allograft survival. *Am. J. Transplant.* 2013. **13**: 1168–1180.

49 **Bishop, D. K.**, **Li, W.**, **Chan, S. Y.**, **Ensley, R. D.**, **Shelby, J.** and **Eichwald, E. J.**, Helper T lymphocyte unresponsiveness to cardiac allografts following transient depletion of CD4-positive cells. Implications for cellular and humoral responses. *Transplantation* 1994. **58**: 576–584.

50 **Schiechl, G.**, **Hermann, F. J.**, **Rodriguez Gomez, M.**, **Kutzi, S.**, **Schmidbauer, K.**, **Talke, Y.**, **Neumayer, S.** et al., Basophils Trigger Fibroblast Activation in Cardiac Allograft Fibrosis Development. *Am. J. Transplant.* 2016. **16**: 2574–2588.

51 **Wakim, L. M.** and **Bevan, M. J.**, Cross-dressed dendritic cells drive memory CD8+ T-cell activation after viral infection. *Nature* 2011. **471**: 629–632.

52 **Gajewski, T. F.**, **Corrales, L.**, **Williams, J.**, **Horton, B.**, **Sivan, A.** and **Spranger, S.**, Cancer Immunotherapy Targets Based on Understanding the T Cell-Inflamed Versus Non-T Cell-Inflamed Tumor Microenvironment. *Adv. Exp. Med. Biol.* 2017. **1036**: 19–31.

53 **Broz, M. L.**, **Binnewies, M.**, **Boldajipour, B.**, **Nelson, A. E.**, **Pollack, J. L.**, **Erle, D. J.**, **Barczak, A.** et al., Dissecting the tumor myeloid compartment reveals rare activating antigen-presenting cells critical for T cell immunity. *Cancer Cell* 2014. **26**: 638–652.

54 **Ruffell, B.**, **Chang-Strachan, D.**, **Chan, V.**, **Rosenbusch, A.**, **Ho, C. M. T.**, **Pryer, N.**, **Daniel, D.** et al., Macrophage IL-10 blocks CD8+ T cell-dependent responses to chemotherapy by suppressing IL-12 expression in intratumoral dendritic cells. *Cancer Cell* 2014. **26**: 623–637.

55 **Brewitz, A.**, **Eickhoff, S.**, **Dahling, S.**, **Quast, T.**, **Bedoui, S.**, **Kroczek, R. A.**, **Kurts, C.** et al., CD8(+) T Cells Orchestrate pDC-XCR1(+) Dendritic Cell Spatial and Functional Cooperativity to Optimize Priming. *Immunity* 2017. **46**: 205–219.

56 **Ohta, T.**, **Sugiyama, M.**, **Hemmi, H.**, **Yamazaki, C.**, **Okura, S.**, **Sasaki, I.**, **Fukuda, Y.** et al., Crucial roles of XCR1-expressing dendritic cells and the XCR1-XCL1 chemokine axis in intestinal immune homeostasis. *Sci. Rep.* 2016. **6**: 23505.

57 **Bottcher, J. P.**, **Bonavita, E.**, **Chakravarty, P.**, **Blees, H.**, **Cabeza-Cabrerizo, M.**, **Sammicheli, S.**, **Rogers, N. C.** et al., NK Cells Stimulate Recruitment of cDC1 into the Tumor Microenvironment Promoting Cancer Immune Control. *Cell* 2018. **172**: 1022–1037 e1014.

58 **Picco, G.**, **Beatson, R.**, **Taylor-Papadimitriou, J.**, **Burchell, J. M.**, Targeting DNGR-1 (CLEC9A) with antibody/MUC1 peptide conjugates as a vaccine for carcinomas. *Eur. J. Immunol.* 2014. **44**: 1947–1955.

59 **Caminschi, I.**, **Proietto, A.**, **Ahmet, F.**, **Kitsoulis, S.**, **Shin Teh, J.**, **Lo, J. C.**, **Rizzitelli, A.** et al., Lew The dendritic cell subtype-restricted C-type lectin Clec9A is a target for vaccine enhancement. *Blood* 2008. **112**: 3264–3273.

60 **Corry, R. J.**, **Winn, H. J.** and **Russell, P. S.**, Primarily vascularized allografts of hearts in mice. The role of H-2D, H-2K, and non-H-2 antigens in rejection. *Transplantation* 1973. **16**: 343–350.

61 **Wood, S. C.**, **Lu, G.**, **Burrell, B. E.** and **Bishop D. K.**, Transplant acceptance following anti-CD4 versus anti-CD40L therapy: evidence for differential maintenance of graft-reactive T cells. *Am. J. Transplant.* 2008. **8**: 2037–2048.

62 **Cossarizza, A.**, **Chang, H.-D.**, **Radbruch, A.**, **Acs, A.**, **Adam, D.**, **Adam-Klages, S.**, **Agace, W. W.** et al., Guidelines for the use of flow cytometry and cell sorting in immunological studies (second edition). *Eur. J. Immunol.* 2019. **49**: 1457–1973.

Abbreviations: **CAR**: chronic allograft rejection · **CTL**: cytotoxic CD8$^+$ T cell · **DAMP**: damage-associated molecular pattern · **DNGR-1**: DC NK lectin group receptor-1 · **MAG**: myelin-associated glycoprotein

Full correspondence: Stefan M. Brunner MD, Department of Surgery, University Medical Center Regensburg, Franz-Josef-Strauss-Allee 11, 93053 Regensburg, Germany.
Email: Stefan.Brunner@ukr.de

The peer review history for this article is available at https://publons.com/publon/10.1002/eji.201948501

Received: 23/12/2019
Revised: 12/5/2020
Accepted: 2/7/2020
Accepted article online: 8/7/2020

© 2020 The Authors. *European Journal of Immunology* published by WILEY-VCH Verlag GmbH & Co. KGaA, Weinheim.

15214141, 2020, 12, Downloaded from https://onlinelibrary.wiley.com/doi/10.1002/eji.201948501 by Open Access University of Augsburg - Universitätsbibliothek Augsburg , Wiley Online Library on [04/05/2026]. See the Terms and Conditions (https://onlinelibrary.wiley.com/terms-and-conditions) on Wiley Online Library for rules of use; OA articles are governed by the applicable Creative Commons License